Journal of Hydrology (NZ) 38(1): 1-28, 1999

A model for determining thresholds for initiation of shallow landslides under near-saturated conditions in the East Coast region, New Zealand

J.C. Ekanayake and C.J. Phillips
Landcare Research, PO Box 69, Lincoln, Canterbury, New Zealand

Abstract

Tephra-covered pastoral hillslopes in the East Coast region of the North Island, New Zealand, are prone to shallow landslides during rainstorms. Past records of climatic and soil hydrological conditions suggest that many of these shallow landslides could have been triggered under near-saturated conditions. The prime cause is most likely to be soil-strength reduction as moisture content changes from unsaturated to saturated after the wetting front reaches the critical shear plane. Approximate thresholds for triggering shallow landslides may be predicted if the time that the wetting front reaches the critical shear plane is estimated for a given set of climatic variables. This paper presents the development of an easy-to-use model to obtain different combinations of rainfall thresholds, slope angles and soil hydraulic properties that would initiate shallow landslides on pastoral hill country in the East Coast region. We assume that the landslide could be triggered when the soil becomes saturated as the wetting front approaches the critical shear plane. The model incorporates a slope-stability model to locate the critical shear plane and a rainfall-infiltration model to estimate the time for the wetting front to reach this critical plane. The application of this model is demonstrated using easily measured field and laboratory soil hydraulic parameters for a hillslope in the East Coast region.

Introduction

Landslides are a common form of erosion in steep hill country in New Zealand (Eyles, 1983). Widespread shallow translational landslides (soil slips or debris flows) have been associated with severe storms, and with the removal of indigenous forest and conversion to grassland for pastoral farming. There have been at least five landslide-causing storms in the last two decades in the East Coast region of the North Island (Fig. 1). Analysis of

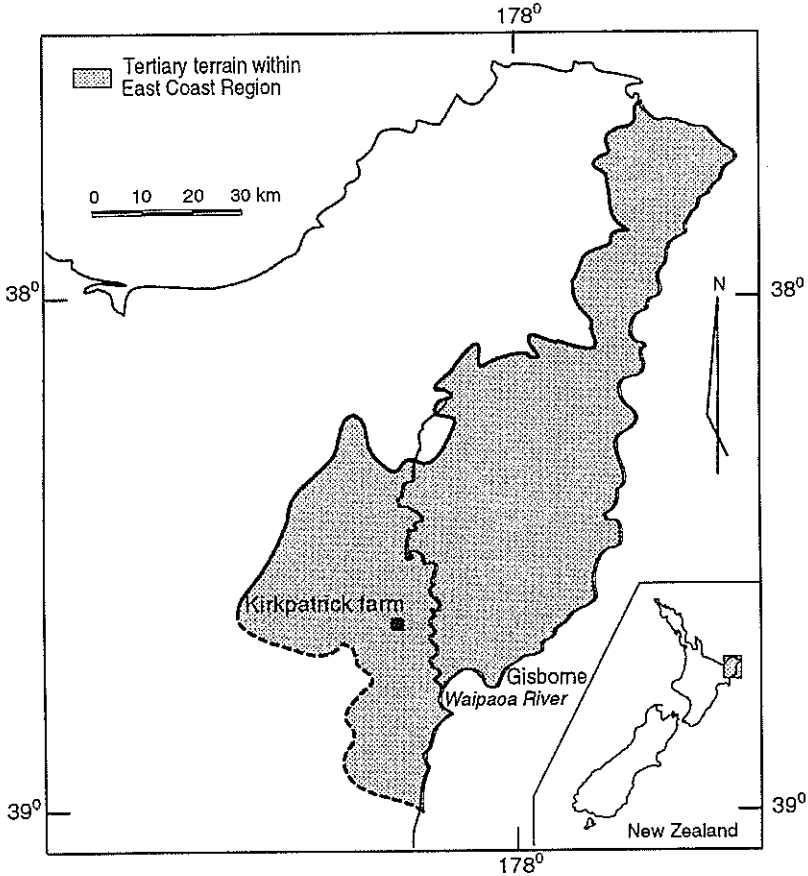

Figure 1 – The East Coast Region of the North Island, New Zealand.

twenty-nine extreme floods in the Waipaoa River since 1900 indicate that there is a greater than 90% probability of an extreme flood occurring in a ten-year period (Kelliher *et al.*, 1995). As regional landsliding is usually associated with these floods, the frequencies of these floods have been used to construct a landslide risk model (Kelliher *et al.*, 1995; Watson *et al.*, in press).

Rainfall-induced, positive pore-water-pressure build up in soil is a well-known cause of many landslides. However, evidence exists that shallow landslides have been triggered even before pore water pressure has begun to build up at the critical shear plane (Wolle and Hachich, 1981; Brooks and Anderson, 1995; Rahardjo *et al.*, 1996; Fourie, 1996). To prove that shallow landslides can be triggered under near-saturated conditions, it is neces-

sary to know the timing of landslide events, and the related climatic data and the antecedent conditions. While previous studies examining landslide-triggering thresholds in New Zealand are based mainly on correlation of climatic data with the landslides (Crozier, 1989; de Rose, 1994) little work has been done on the triggering thresholds for shallow landslides under near-saturated conditions (Brooks *et al.*, 1998).

Climatic data are available for previous landslide-causing events in the East Coast region, but there are no details on the times the landslides were triggered, so we cannot estimate soil moisture conditions at the time of failure. We can, however, estimate the minimum rainfall required to just saturate the soil regolith over the critical shear plane, by assuming a uniform antecedent moisture content equivalent to field capacity (a volumetric moisture content of soil at -200 cm tension of 34%) for the whole soil depth above the shear plane. The difference between the recorded rainfall and the calculated minimum rainfall required to saturate the soil regolith can then be used to find the approximate degree of saturation of the soil at the time of failure. Although the estimates are crude because of assumptions of high antecedent soil moisture and negligible water losses due to evapotranspiration, surface runoff, and drainage, such calculations show the possibility of shallow landslides being triggered under near-saturated conditions. Examples of this phenomenon can be seen in landslides occurring during storms in Taranaki, a region which has similar characteristics to the East Coast (de Rose, 1994;Table 1).

Although rainfall is a prime factor in the triggering of landslides, prediction of the rainfall thresholds needed to trigger them depends not only on climatic variables but also on soil characteristics and the magnitude and direction of forces in the hillslope influenced by water infiltration. This suggests that models to predict the threshold conditions for triggering landslides must incorporate models for both rain water infiltration and slope-stability. In this paper we present an easy-to-use combined model to find different combinations of threshold conditions of rainfall, antecedent soil moisture, and slope angle for triggering shallow landsliding under near-saturated conditions on pastoral hillslopes in the East Coast region of the North Island, New Zealand.

Model development

General study area characteristics

The East Coast hill country has a number of factors that predispose it to landsliding. Its geology is largely alternating sequences of mudstones and sandstones of Tertiary age (Moore and Mazengarb, 1992). Porous tephra cover beds, 30 to 100 cm thick, overlie low permeability bedrock colluvium and impermeable bedrock. This airfall and reworked tephra, derived from

Table 1 – Required minimum rainfall to saturate the soil regolith over the shear plane and recorded rainfall totals for Taranaki (reproduced from de Rose, 1994).

Event	Recorded total rainfall	Minimum total rainfall required to fill the soil water store between Field Capacity and saturation for soil of 75 cm depth	No. of landslides	Mean size of landslides
	(mm)	(mm)		(m^2)
6 Dec 1968	128	157		
24 Feb 1971	227	157	100	92
23 July 1974	135	157		
28 June 1975	113	157		
7 May 1979	110	157	29	27
10–11 Dec 1982	108	157	63	40
22–23 Jan 1987	83	157	91	70
29 Jan 1990	120	157		
9–10 Mar 1990	235	157	371	88

the Taupo volcanic zone, forms a surface soil layer of variable composition and thickness over the colluvial layer in most parts of the East Coast region. For convenience we do not differentiate individual tephra but treat the soil as two distinct layers. The boundary between the tephra and colluvium layers is distinct and easily identified in the field. Although both layers showed high shear strength under field moisture content (undrained field vane shear test > 80 kPa), often shear strength reduced to as low as 2 kPa when the layers became saturated. Records of past landslide scars suggest that most of the shear planes of the slope failures lie within the basal tephra or colluvium beds (in't Veld and de Graaf, 1990). As a result, soil hydrology and slope stability can be analysed on the basis of two soil layers. To

generalise our approach for other two-layered soils, the upper soil is referred to as layer-1 and the lower as layer-2.

Existing models

Physically-based models combining both hydrology and slope stability are not new. Current models employ a range of analytical methods, including finite differences (Brooks *et al.*, 1993; Anderson and Lloyd, 1991) grid-based approaches (Montgomery and Dietrich, 1994), Digital Elevation Model (DEM)-GIS approaches (Murillo and Hunter, 1996), and others. A problem with many of these models is the amount of data required to run them and the difficulty of establishing relationships between the hydraulic and strength properties of soil. Our approach is to use easily measured field and laboratory parameters to determine the thresholds for triggering landslides.

The slope-stability model

The purpose of the slope-stability model as used in this study is to locate the critical shear plane(s). For stability analysis, hillslopes in the East Coast region may be regarded as uniform and "long" in relation to the depth of failure. The shape of the failure surface is generally planar, so the stability of these hillslopes can be analysed as infinite slopes using the limit equilibrium method (Lambe and Whitman, 1979). The strength contributed by pasture plant roots is not considered in the stability model. Two major forces are considered in limit equilibrium analysis: actuating forces (that create the soil shear stress) and resisting forces (that create the soil shear strength).

Soil stresses are created by the soil weight, the amount of moisture held in the pore spaces, and the angle of the slope upon which the soil rests. Soil stress is estimated by measuring the slope angle, soil or regolith thickness over the shear plane, and field soil bulk density. Soil shear strength is determined mainly by the magnitude of soil strain associated with soil-water interactions and the physical and chemical properties of the soil. The actual shear strength used in the stability analysis depends on the current activity of the landslide, which is determined by the shear strain in the soil at the shear plane at the time. Shear strength corresponding to the peak of the stress-strain curve is used here, as we focus only on the triggering of landslides.

Soil shear strength may be estimated using either "effective" or "total" strength parameters according to the Mohr-Coulomb failure criteria (Lambe and Whitman, 1979). To use effective strength parameters in stability analysis, the pore-water pressure at failure must also be known. This requirement makes effective stress analysis difficult to apply in the unsteady conditions associated with soil hydrology in natural hillslopes during rain. In

some analyses, the pore-water pressure is assumed to correspond to a water table at the soil surface. This leads to an estimate for the safety factor that is lower than the actual value if the real water table is below the slope surface.

The rate of climatic loading of natural hillslopes can be considered to be much faster than the time required for soil consolidation and pore-water dissipation. If a landslide is triggered under such conditions of negligible change in water content, "total" strength parameters (Φ=0 or undrained shear strength) are more appropriate than "effective" strength parameters in stability analysis (Lambe and Whitman, 1979). The advantage of using undrained shear strength is that the pore-water pressure need not to be known for stability analysis. We used undrained shear strength in our stability model.

Because of its simplicity and reliability within its limitations (Chandler, 1988), field-vane-shear results, corrected by the Bjerrum (1973) correction factor μ (easily obtained from the Plasticity Index), have been used to estimate the undrained shear strength for our stability model. There are a number of assumptions in our approach. These are:

1. Soil failure is assumed to occur at near-saturation, when the wetting front reaches the critical shear plane.
2. The pore-water pressure at the wetting front is assumed to be zero.
3. The strength contribution due to soil shear strength from the pasture plant roots is assumed to be negligible.

The average saturated field bulk density of the corresponding soil layer is used to calculate the soil shear stress.

Safety factor and critical depth

The safety factor (S.F.) determined from the limit-equilibrium infinite-slope-stability analysis (Fig. 2) using the corrected field-vane-shear results is given by Equation 1:

$$(S.F.) = \frac{\mu_2 S_{u2}}{[\gamma_1 Z_1 + \gamma_2 (Z_{cr} - Z_1)] Sin(\alpha) Cos(\alpha)} \qquad (1)$$

where S_{u2} is the undrained shear strength of soil layer-2 obtained from the vane shear apparatus, and μ_2 is the Bjerrum (1973) correction factor for soil layer-2; γ_1 and γ_2 are the average saturated field bulk densities of layer 1 and layer 2, respectively; α is the slope angle; and Z_{cr} is the location of the critical shear plane measured from the soil surface, with Z_1 being the thickness of the first soil layer. The location of the critical shear plane measured from the surface using the corrected-vane-shear strength is then given by Equation 2. This relationship is obtained by assuming the critical shear plane is always located below soil layer-1.

$$Z_{cr}=[\ \frac{\mu_2 S_{u2}}{\gamma_2 Sin(\alpha)Cos(\alpha)} - (\frac{\gamma_1}{\gamma_2} - 1)Z_1] \qquad (2)$$

If layer-1 is thick enough for the critical shear plane to form in layer-1, its location is given by Equation 3:

$$Z_{cr}=[\frac{\mu_1 S_{u1}}{\gamma_1 Sin(\alpha)Cos(\alpha)}] \qquad (3)$$

where S_{u1} is the undrained shear strength of layer-1 obtained from the vane shear apparatus, and μ_1 is the Bjerrum correction factor for layer-1.

To evaluate the location of the critical shear plane determined by the vane shear apparatus, effective-shear-strength parameters, determined under labo-

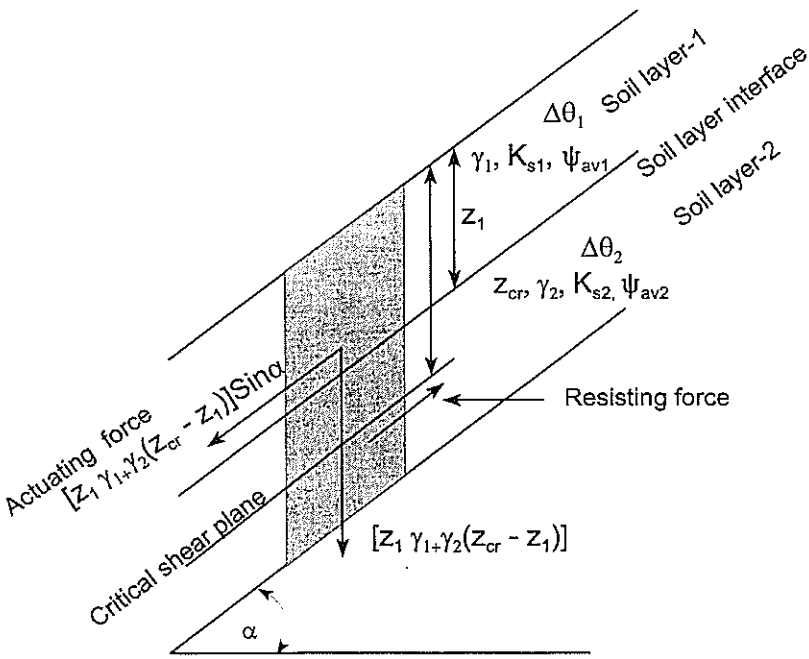

Figure 2 – Forces used in limit equilibrium analysis for a two-layered, vertical soil column within an infinite slope. $\Delta\theta_1$ and $\Delta\theta_2$ are the differences between initial and saturation moisture contents of two soil layers, K_{s1} and K_{s2} are saturated hydraulic conductivities, γ_1 and γ_2 are field bulk densities, ψ_{av1} and ψ_{av2} are average suction at wetting front of two soil layers, Z_1 is the thickness of soil layer-1, and Zcr is the depth to the critical shear plane from the surface.

ratory conditions from direct shear tests of remoulded soil samples, were also used to find the critical shear plane, using Equations 4 and 5:

$$(S.F) = \frac{[C_2' + (\gamma_1 Z_1 + \gamma_2 (Z_{cr} - Z_1))\alpha - Z_{cr}\gamma_w] Cos^2(\alpha) \tan\phi_2'}{[\gamma_1 Z_1 + \gamma_2 (Z_{cr} - Z_1)] Sin(\alpha) Cos(\alpha)} \quad (4)$$

where Z_{cr} is the location of the critical shear plane measured from the soil surface and γ_w is the unit weight of water, and C_2' and ϕ_2' are the effective cohesion and angle of friction of layer-2, respectively. Equation 4 is derived by assuming that the critical shear plane is located within layer-2. Since the level of the water table is not known, it is assumed to be at the soil surface. After rearranging Equation 4, the critical depth for the hillslope, Z_{cr}, is then given by Equation 5:

$$Z_{cr} = \frac{C_2' + [(\gamma_1 - \gamma_2) Cos(\alpha) \tan(\phi_2') - Sin(\alpha)] Z_1 Cos(\alpha)}{\gamma_2 Cos(\alpha) Sin(\alpha) - (\gamma_2 - \gamma_w) Cos^2(\alpha) Tan(\phi_2')} \quad (5)$$

As layer-1 depth increases, the critical shear plane moves towards the soil layer interface. If the location of the critical shear plane shifts into layer-1, its location is given by Equation 6:

$$Z_{cr} = \frac{C_1'}{\gamma_1 Cos(\alpha) Sin(\alpha) - (\gamma_1 - \gamma_w) Cos^2(\alpha) Tan(\phi_1')} \quad (6)$$

where C_1' and ϕ_1' are the effective cohesion and angle of friction for the first soil layer.

Effective strength parameters measured in the laboratory were then used in Equations 5 and 6 to estimate the locations of critical shear planes to compare with the planes determined from the vane shear tests.

The rainwater infiltration model

Once the approximate location of the critical shear plane is found, the timing of the critical threshold for hillslope instability in relation to climatic conditions may be predicted if the rate of wetting-front advance is known. This can be estimated from the water infiltration model. The Richard's equation is regarded as the best method to approximate the wetting-front advance in unsaturated soil, and many solutions have been developed based on numerical and analytical methods (Hillel, 1977). However, these solutions are not easy to apply, as the relationship between hydraulic conductivity and soil moisture content needs to be determined.

The Green and Ampt (1911) infiltration model can be used to approximate the rate of the wetting-front advance in uniform and layered soil (Childs and Bybordi, 1969; Whisler and Bouwer, 1970; Mein and Larson, 1973; Kao and Hunt, 1996). Pradel and Raad (1993) have used this model to time the wetting-front advance to the critical shear plane in hillslopes. Compos-

ite models to predict thresholds of landslides under near-saturated conditions have been developed by linking finite-difference infiltration models with slope stability models (Anderson and Howes, 1985; Anderson and Lloyd, 1991). Application of these infiltration models to shallow landslides is, however, limited by the difficulty of establishing relationships between hydraulic conductivity and moisture content, and soil strength parameters.

In our model, we chose an improved version of the Green and Ampt model that predicts the timing of the wetting-front advance in hillslopes with layered soils (Mein and Larsen, 1973). When rainfall intensity is greater than the saturated hydraulic conductivity of the soil, the soil surface becomes saturated, and at some stage runoff begins to be generated over the soil surface (Mein and Larson, 1973). If the rainfall intensity is always less than the saturated hydraulic conductivity, all the water will infiltrate into the soil. In using this approach we make the following assumptions:

1. Soil regolith is uniform and rainwater reaches the shear plane only by infiltration.
2. The average uniform rainfall intensity (i) is larger than the saturated hydraulic conductivity of the soil layer-1(K_{s1}).
3. The saturated hydraulic conductivity of soil layer-2 (K_{s2})is smaller than the saturated hydraulic conductivity of soil layer-1(K_{s1}).
4. The antecedent moisture content is uniform through the soil profile.

We now consider a thin vertical soil column on an earth slope (Fig. 2). If the initial moisture content, (θ_{1i}) of layer-1 is assumed to be uniform through the soil depth, the infiltration rate f(t), after time t of rain starting, can be approximated by Equation 7 (Green and Ampt, 1911; Mein and Larson, 1973):

$$f(t) = \frac{dF(t)}{dt} = K_{s1}\left[1 + \frac{\psi_{av1}\Delta\theta_1}{F(t)}\right] \tag{7}$$

where K_{s1} is the saturated hydraulic conductivity of the soil, F(t) is the cumulative infiltration after time t since the rain began, ψ_{av1} is the average capillary suction at the wetting front, and $\Delta\theta_1$ is given by (θ_{s1}-θ_{i1}) where the saturated and initial moisture content of layer-1 are $\theta_{s1}$and θ_{i1} respectively. If the rainfall intensity is higher than the saturated hydraulic conductivity, the time t_s for runoff to begin after surface saturation is given by Equation 8:

$$t_s = \frac{K_{s1}\psi_{av1}\Delta\theta_1}{i(i-K_{s1})} \tag{8}$$

where the uniform rainfall intensity is given by i. Equation 7 can be integrated to find the critical time t_{cr1} when the wetting-front reaches a critical depth Z_{cr} within layer-1 and is given by Equation 9:

$$t_{cr1} = [Z_{cr} - Z_s - \psi_{av1} \ln \frac{[\psi_{av1} + Z_{cr}]}{[\psi_{av1} + Z_s]}] \frac{\Delta\theta_1}{K_{s1}} + t_s \tag{9}$$

where ψ_{av1} is the average capillary suction at the wetting-front advance, K_{s1} is the saturated hydraulic conductivity of soil layer-1, i is the rainfall intensity, and Z_s is the saturation depth. Note that i must be greater than K_{s1} for surface runoff to start. If i is less than K_{s1} the soil surface will not become saturated and the Green and Ampt model cannot be used to estimate the rate of the wetting-front advance.

If the critical depth is located in layer-2, Equation 9 can be further extended to approximate the timing for the wetting front to reach the critical depth Z_{cr} in layer-2, as given in Equation 10 (Childs and Bybordi, 1969):

$$t_{cr2}=(Z_{cr}-Z_1)\frac{\Delta\theta_2}{K_{s2}}+\frac{1}{K_{s1}K_{s2}}[\Delta\theta_2(Z_1K_{s2})-K_{s1}(\psi_{av2}+Z_1)]\ln[1+\frac{(Z_{cr}-Z_1)}{(\psi_{av2}+Z_1)}]+t_1 \quad (10)$$

where $\Delta\theta_2 = (\theta_{2s}-\theta_{i2})$, θ_{2s} is the saturated moisture content of layer-2 and θ_2 is the initial moisture content of layer-2, assumed to be uniform along the soil depth, t_1 is the time taken for the wetting front to reach the soil layer interface, which is Z_1 below the soil surface (thickness of layer-1) and can be found from Equation 9 by substituting $t_{cr1} = t_1$ and $Z_{cr} = Z_1$, and ψ_{av2} is the average capillary suction at the wetting front in layer-2. This is valid as long as the saturated hydraulic conductivity, K_{s2}, of layer-2 is smaller than the saturated hydraulic conductivity, K_{s1}, of layer-1. Generally this assumption is valid for most hillslopes in the area because the colluvium layer has a lower saturated hydraulic conductivity than the overlying loose layer-1.

As different soil layers are involved in the model development, the saturated hydraulic conductivity of the soil must be measured at different depths. We used the Guelph permeameter, as it may be used to measure the saturated hydraulic conductivity of soil if a sufficient number of measurements are taken (Gupta *et al.*, 1993). With this instrument, the one-head method (Elrick *et al.*, 1989) was used, due to its simplicity and applicability to different soil depths.

To approximate the average wetting-front suction for use in the infiltration model, Brakensiek's (1977) method was used, as it is simple and requires only the moisture release curve information to determine the wetting-front suction. Porosity was calculated from field bulk density, and volumetric moisture content measured using the field test methods and standard particle density.

Model verification - field study

Model verification demands physical evidence of the time when the rainfall-induced wetting front reaches the critical depth of a hillslope. An experimental plot (7 m x 15 m) on a south-facing upper slope was selected on a pastoral farm approximately 20 km south of Gisborne (Kirkpatrick farm) (Fig. 1). This farm, along with most others in the region, had experienced

several episodes of landsliding in the last few decades. Much of the land cleared for pastoral farming comprises dissected, steep hill country with slopes of 25 – 40°. The steep hill country is underlain by a sequence of competent late-Tertiary sedimentary rocks (mainly fine sandstone). These rocks support steep valley slopes where shallow translational landslides (debris avalanches and flows or soil slips) are the dominant erosion process.

Most soil slips in the vicinity of the study area occur on slopes between 20° and 32°, with most in mid- to upper slope positions. Tephra over colluvium was the predominant material exposed in the head wall scarps of 576 erosion features examined in a study following Cyclone Bola (in't Veld and de Graaf, 1990). Our own observation of landslides throughout the region also indicates that the slope position at which failure occurs is often associated with changes in subsurface soil characteristics, such as thinning of the tephra and convergent subsurface flow pathways.

To check the validity of our rainfall infiltration model, we installed an automatic data-logging system to measure changes in the soil-moisture profile during rain, to compare the estimated and observed wetting-front advance rate. The automatic data-logging system included 44 tensiometers (Fig. 3) with temperature-compensated, differential, piezo-resistive pressure transducers, a tipping-bucket raingauge, temperature probes, and a CR10X (Campbell Scientific Instrument) data-logger with an AM4x16 multiplexer. The whole system was powered by a 12-V battery supplemented by solar power. A cellphone was used to communicate between the Gisborne field site and the Landcare Research office at Lincoln. Averages of 40 readings of the soil water potentials at each tensiometer cup were measured at 30-min intervals, and recorded with the 30-min rainfall totals. Daily rainfall totals, battery voltage, and temperature, were recorded every midnight. Data were down-loaded every fortnight. Tensiometers were purged (de-aired) without being removed if they became dry during dry periods, when suctions exceeded -700 cm of water. An example of typical tensiometer responses to rainfall is shown in Figure 4.

A total of 21 tests of saturated hydraulic conductivity were made, three along each soil profile at depths 10, 50, and 100 cm (Table 2). Field bulk densities were measured using 10 x 10 cm stainless steel cores and a portable electronic scale. Water contents of the field soil were measured before the cores were extracted using a Time Domain Reflectometer. Three tests were made at each depth giving a total of 36 tests at four locations 1.5 m apart along the experimental plot.

The vane shear test was run in conjunction with the Guelph permeameter test to obtain the shear strength of the saturated, undrained soil. A Pilcon direct vane shear tester was used to measure the soil shear strength along four soil profiles within the experimental plot. A 33-mm diameter vane was

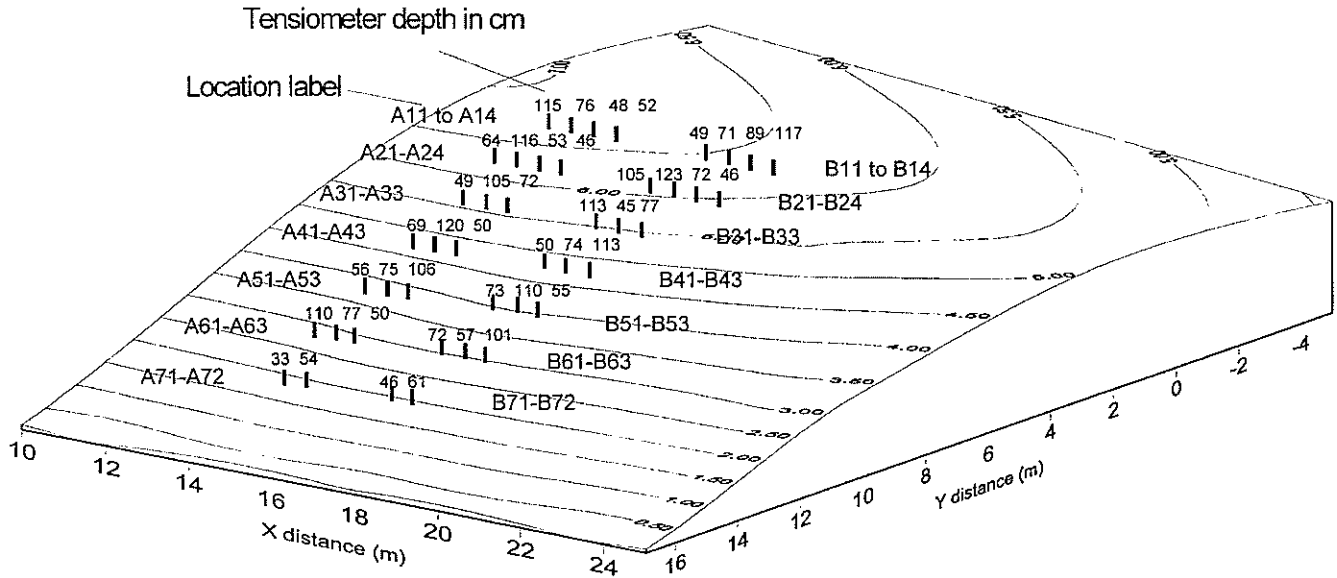

Figure 3 – Study site, Kirkpatrick farm, Gisborne locations of tensiometers and their depths.

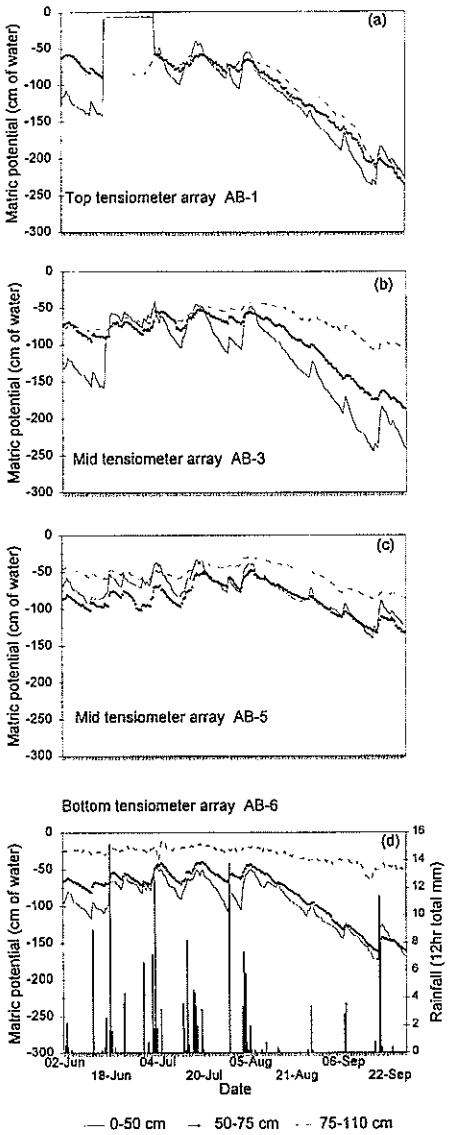

Figure 4 – (a-c) Tensiometer data (cm of water) during the period June - September 1996. Data for top, mid, and bottom tensiometer arrays; (d) 12-hour-rainfall totals for June - September 1996.

Table 2 – Summary of the average soil physical parameters obtained from field and laboratory tests.

Soil layer	K_s m/day (mm h^{-1})	γ_{sat} kN/m^3	η %	ψ_{av} cm	ϕ' Deg	C' kPa
soil layer-1	0.134 (5.6)	16.3	55	16	16	6.8
soil layer-2	0.112 (4.7)	17.2	48	27	12	4.5

K_s = saturated hydraulic conductivity(m/day)
γ_{sat}= saturated soil bulk density (kN/m^3)
η= porosity (%)
ψ= average capillary suction at the wetting front (cm)
ϕ'= effective angle of friction (degree)
C' = effective cohesion (kPa)

used in saturated soil and a 19-mm vane was used in unsaturated soil. The vane was gently inserted about 5 cm into the saturated soil at the bottom of the hole just after the saturated hydraulic conductivity was measured. It was rotated at an approximate strain rate of 6^0 sec^{-1} until the soil failed. The unsaturated soil strength was measured at a similar depth and close to the hole used to measure the saturated strength. The field moisture content of the unsaturated soil was determined using the Time Domain Reflectometer.

Laboratory tests

Moisture release curves were used to estimate the average suction head at the wetting front. Three average moisture-release-curves for soil depths 0–20, 20–50, and 50–100 cm were obtained using a standard pressure-plate apparatus. A total of 42 soil samples were used for a suction range of 0 to 500 cm water in steps of 100-cm water suction.

Effective strength parameters (cohesion and angle of friction) were determined from 18 remoulded soil samples at three arbitrary moisture contents from unsaturated to saturated using a constant rate, direct shear apparatus. The liquid limit and the plastic limits were also determined (Lambe, 1951) and the soil plasticity index was then used to correct the field vane-shear-test data.

Results and discussion

Triggering of landslides under near-saturated conditions

Our model is developed on the assumption that the shallow landslides in the tephra-covered pastoral hillslopes are most likely to be triggered under near-saturated conditions. Although landslide failure is commonly attributed to saturated conditions arising from heavy rainstorms, some evidence

exists to show that landslides can be triggered under near-saturated conditions (Wolle and Hachich, 1981; Brooks and Anderson, 1995; Rahardjo *et al.*, 1996; Fourie, 1996).

While it is difficult for us to prove that landslides can occur under near-saturated conditions in our study area because of insufficient data and the lack of a triggered landslide, we can however estimate approximate field soil moisture conditions at the time of landslides by using the recorded rainfall and assumed antecedent soil moisture conditions. The minimum rainfalls required to saturate the soil regolith given in Table1 are estimated by assuming an antecedent field moisture content at field capacity (34% (vf) at -200 cm water tension). If the recorded rainfall is less than this required minimum, we assume that the soil regolith is still unsaturated at the time of failure. However, this estimate still does not tell us the exact pore-water pressure at the critical shear plane at the time of failure.

On many occasions, during field soil shear testing in the study area, we have noticed a significant drop in soil shear strength following wetting of the soil. These observations, and the examples given in Table1, led us to conclude that shallow landslides may be triggered in near-saturated conditions in areas similar to the study area. Our model predictions are estimated by assuming that the failure could occur when the unsaturated soil at the critical shear plane reaches saturation, as the infiltrating rainwater approaches the critical shear plane.

Model parameters

Saturated hydraulic conductivities were measured at different depths at four locations in the experimental plot (Fig. 5a) and field bulk densities were represented as averages of three at each depth. Uncorrected field-vane-shear strengths are given for different depths, at their field moisture contents and after saturation in Figure 5b, and the Bjerrum correction factor vs. plasticity index in Figure 5c. Moisture release curves were obtained for soil from three different depth ranges (Fig. 6a), with the average effective cohesion and angle of internal friction from direct shear tests presented for three moisture contents (Fig. 6b and Table 2), and the liquid and the plastic limits for two depths (Fig.6c and Table 2).

Critical shear plane location

Location of the critical shear plane can be estimated if the slope angle and the soil layer thickness are known (Fig. 7a). The location of the critical shear plane varied with the depth of layer-1 and with the shear strengths of the two soil layers (Fig. 7a,b). Figure 7b also shows in detail how the location of critical shear planes obtained from effective-shear-strength parameters vary with the thickness of layer-1. The critical shear planes in this

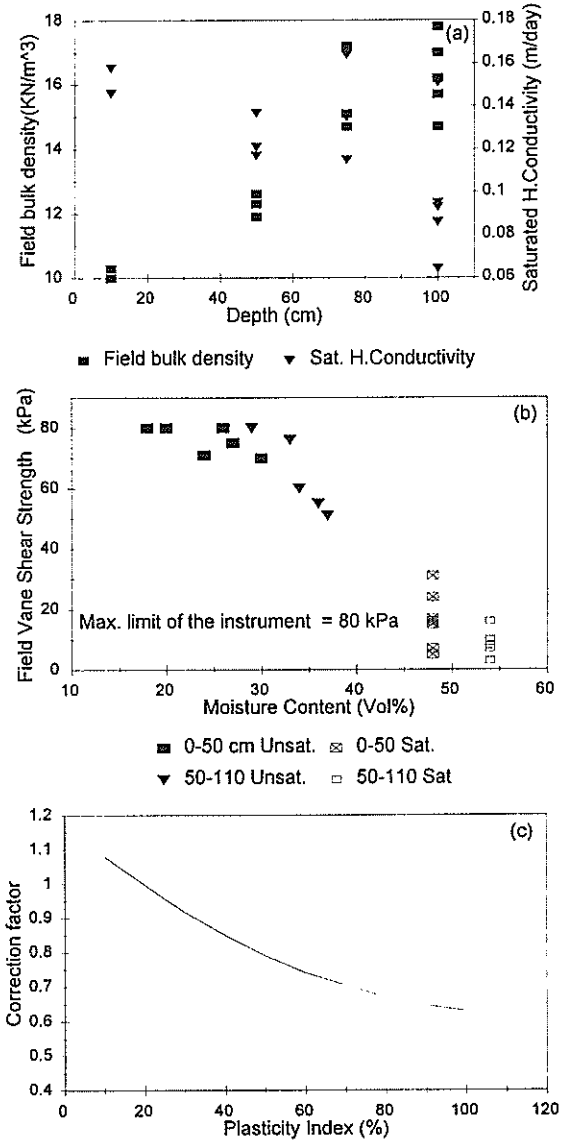

Figure 5 – (a) Variation of field bulk density and saturated hydraulic conductivity with depth.
(b) Saturated and unsaturated vane shear results (undrained soil shear strength) before correction.
(c) Bjerrum correction factor chart (Bjerrum 1973).

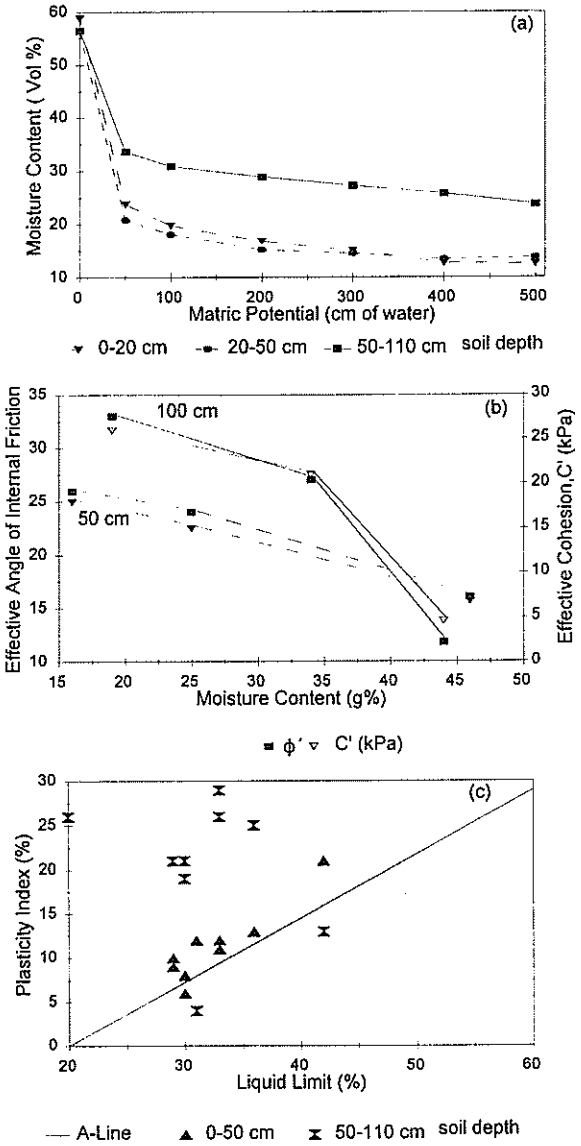

Figure 6 – (a) Moisture release curves for soil at three different depths within the hillslope.
(b) Effective soil strength parameters obtained from the direct shear test.
(c) Plasticity index chart for soils in two soil layers.

case are estimated assuming the worst conditions, i.e., the water table is at the soil surface. The locations of critical shear planes estimated from corrected vane-shear-strengths are shown in Figure 7c. As the thickness of layer-1 increases, the critical shear plane moves towards the soil layer interface (Fig. 7b,c). Because the shear strength of saturated soil in layer-2 was much lower than that for layer-1, the critical shear plane is more likely to be located in layer-2 for a wider range of layer-1 thicknesses. On the other hand, if the shear strength of layer-2 is significantly greater than layer-1, the shear planes of most shallow landslides in the study area would be expected to be found at the interface between the soil layers for a wider range of layer-1 thicknesses. Once the critical shear plane approached the soil layer interface it remained at the interface for further increases in the depth of soil layer-1 (Fig. 7b,c). The extent to which the critical shear plane lay on the soil layer interface depended on the difference in soil shear strength between the two soil layers. Once the location of the critical shear plane moved into layer-1, the strength parameters corresponding to layer-1 were used in Equations 2, 3, 5 and 7 to find the critical depths. Locations of the critical shear plane for hillslopes without a soil layer-1 can be evaluated by substituting $Z_1 = 0$ in Equation 5.

As the most sensitive model parameter is the strength of the undrained soil, strength parameters must be estimated with caution. Use of the field-vane-shear method to calculate the location of critical shear planes appeared to overestimate the critical depth compared with depths estimated using laboratory-derived parameters of effective shear strength (Fig. 7b,c). It is possible, however, that effective strength parameters, measured under laboratory conditions on remoulded soil samples, may well have been underestimated. If effective-shear-strength parameters are used to estimate the depth of the critical shear plane, effective cohesion becomes the most sensitive model parameter. A slight increase in estimated soil strength will significantly increase the depth of the critical shear plane and therefore increase the estimated time of infiltration and the critical rainfall duration.

Theoretical estimates of shear-plane depths, using the infinite-slope, limit-equilibrium method with measured shear strengths, were slightly higher than those observed in the field (Fig. 7a,b,c). For example, for a soil layer-1 thickness of 1.0–1.5m on slopes of 35–45^0, estimates put the critical shear plane about 1m from the soil surface, corresponding to the soil layer interface. However, field observations in and around the study area suggest that the average depth of shear plane for such conditions is around 0.6–0.85m (Phillips *et al.*, 1990). This suggests that the actual loss of soil-shear-strength in the field soil during the saturation process is higher than the measured values.

The different location of the theoretical compared to the actual shear plane

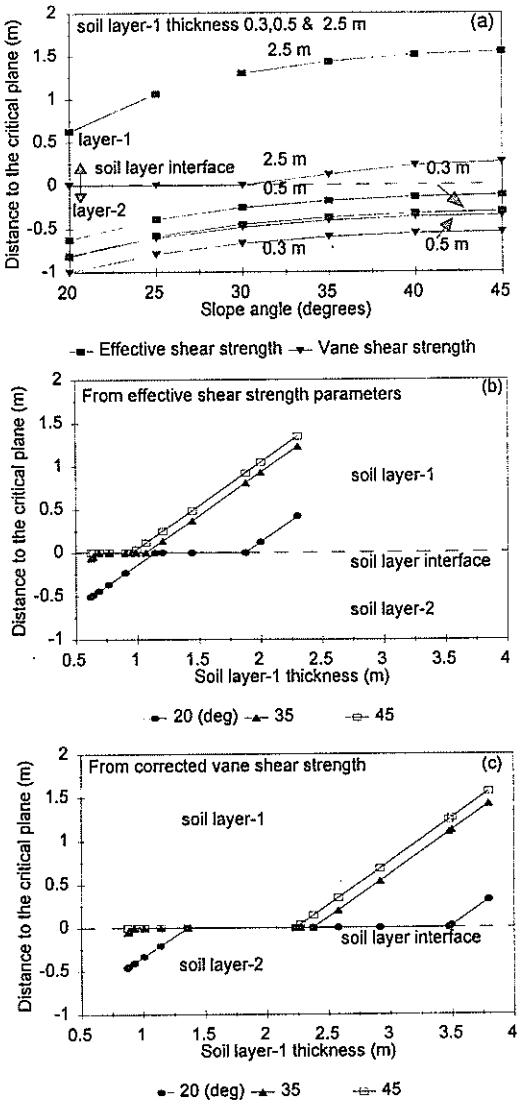

Figure 7 – (a) Locations of critical shear planes for different slopes angles and soil layer-1 thickness obtained from Eqs. 2, 3, 5 and 6.
(b) Locations of the critical shear planes obtained using the effective shear strength parameters in Eqs. 5 and 6.
(c) Locations of the critical shear planes obtained using the corrected vane shear results in Eqs. 2 and 3.
Note that the distances shown are measured from the soil layer interfaces.

may be explained by the abrupt reduction in soil shear strength near saturation. This marked loss of strength, particularly in layer-2, was clearly observed during the field-vane-shear test, as the vane blade effortlessly sank into the saturated layer-2. The laboratory direct-shear tests on saturated, remoulded soil samples also showed this abrupt strength loss. Disintegration of the soil matrix, with an abrupt reduction of soil strength, observed in saturated soil, may support the fluidisation mechanism in soil proposed by Crozier (1969) as a reason for the initiation of shallow landslides. Viscous flow of the soil after losing strength at saturation may well explain the formation of tunnel gullies that occur in tephra in many locations in the East Coast region.

Runoff time, rainfall intensity and antecedent moisture content

The time for runoff to begin after the start of rainfall is a significant part of the total time for the wetting front to reach the critical plane (Fig. 8a). If the average rainfall intensity is less than the saturated hydraulic conductivity of the surface soil, runoff will not be generated. On the other hand, the time for runoff to start could be significantly increased if the rainfall intensity factor is slightly larger than that for saturated hydraulic conductivity, as the magnitude of the numerator of Equation 8 indicates. We can estimate many possible combinations of time for runoff to start and rainfall intensity for various antecedent moisture conditions using Figure 8a. Reduction of antecedent moisture content by 70% at 8 mm/h rainfall intensity increases runoff time by 77%. Runoff time will decrease by 84% if the rainfall intensity is increased from 8 to 14 mm/h at 10% saturation antecedent moisture content. Rainfall intensity has no significant effect on runoff time when the antecedent soil moisture content is closer to saturated conditions (Fig. 8a). For rainfall intensities higher than 14 mm/h, time for the runoff to start also does not depend significantly on the antecedent moisture content.

Triggering threshold combinations

Landslide-triggering thresholds were estimated by substituting depths of critical shear plane from the stability model (Equations 2 and 3) into the rainfall infiltration model (Equations 9 and 10). Since our aim was to use simple model parameters, only critical shear plane depths obtained from the vane shear strengths values (Equations 2 and 3) were used in the rainfall infiltration model, rather than effective strength parameters. The different combinations of rainfall intensity, duration, and slope angle for critical shear planes located within layer-1 (Fig. 8b) were evaluated using Equations 3 and 9. For example, a hillslope with a slope angle of 35^0 at an antecedent moisture content of 50% saturation will become unstable after 82 h of rainfall at a uniform intensity of 11mm/h. If the antecedent moisture content is

increased to 80%, the same hillslope, under similar conditions, will becomes unstable after 34 h.

Combinations of rainfall intensity and duration, antecedent moisture content, and slope angle when the critical shear plane is located in soil layer-2 (Fig. 9a,b) were obtained by substituting the critical shear plane depths from the stability model (Eq. 2) into the infiltration model (Eq.10). Time taken for the wetting front to reach the soil layer interface, t_1, was first determined from Equation 9 using the runoff time, t_s, found from Equation 8. Then

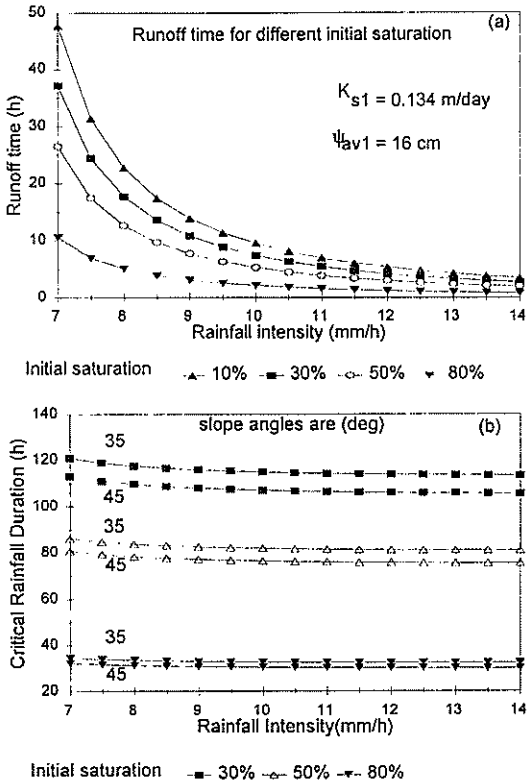

Figure 8 – (a) Time for runoff to start, estimated using Eq. 8, for different rainfall intensities and antecedent moisture contents.
(b) Critical rainfall duration time for slope instability estimated from Eqs. 9 and 10 for slope angles of 35° and 45° when the critical shear plane is located in soil layer-1. Locations of the critical shear planes are estimated from Eqs. 2 and 3 for the slope angles shown.

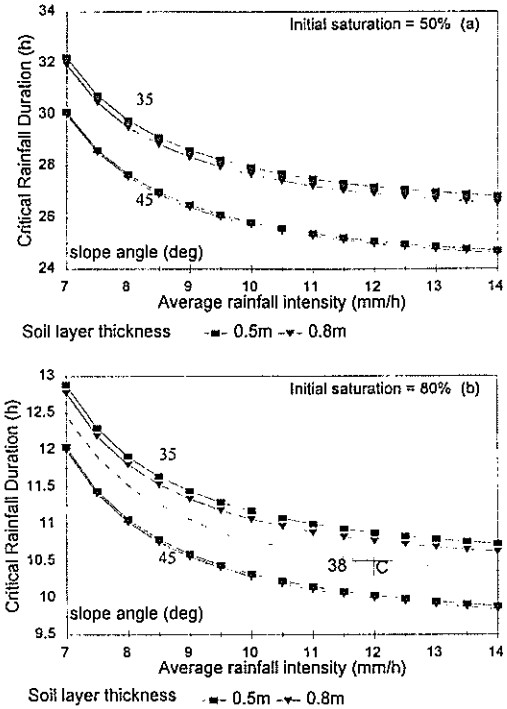

Figure 9 – Critical rainfall durations for different soil layer-1 thicknesses, slope angles and initial moisture contents estimated from Eq. 10.(a) 50% and (b) 80% saturation. Locations of the critical shear planes are estimated from Eq. 2 for shown slope angles. Point C refers to example 2 in Table 4.

Equation 10 was used to find the critical time for the wetting front to approach the critical depths calculated for different combinations of slope angle and strength parameters from Equation 2. These equations can be used to find different combinations of rainfall intensity and critical time duration for slopes to become unstable, if the slope angle and antecedent moisture content are known. For example, a hillslope with a 0.8 m-thick soil layer-1 and a slope angle of 35°, at an antecedent moisture level of 50% , becomes unstable after 29 hours of rainfall at a uniform intensity of 8.5mm/h (Fig. 9a). If the antecedent conditions are changed to 80% saturation, this hillslope becomes unstable after about 11 hours for the same rainfall intensity. The model can be applied by following the outline in Table 3. All calculations can be carried out in a spreadsheet, and the model may be used to produce graphs or nomograms as shown in Figures 7 to 9. Two worked examples are given in Table 4.

Table 3 –Steps to follow in model application

Steps	Technique
1. *Field tests* Saturated hydraulic conductivity - K_s Bulk densities and porosities- γ, η Shear strength parameters - S_u	 Guelph permeameter Soil cores, portable balance, TDR Pilcon or any other vane shear
2. *Laboratory tests* Moisture release curve - ψ - Θ Plasticity index - PI	 Pressure plate apparatus Casagrande apparatus
3. *Calculations* Estimate the average suction at the wetting front for both soil layers from the moisture release curve method as given in Brakensiek (1977) (Fig. 6a) Produce the plasticity index chart (Fig. 6b) Find the appropriate Bjerrum's correction factor from Fig. 5c Calculate the locations of critical shear planes using the corrected field vane shear strength and bulk densities, for a range of necessary slope angles, using Eq. 2 or Eq. 3 (Fig. 7a). Use Eq. 9 to produce Fig. 8b and Eq. 10 to produce Fig. 9(a,b).	

Variable rainfall, ranging from 300 to 900 mm within 3 days, was received in the East Coast during Cyclone Bola in 1988 (Phillips *et al.*, 1990). This is approximately equivalent to a 4 to 12.5 mm/h average rainfall over 72 h. Almost all slopes greater than 35^0 and with soil layer-1 thicknesses greater than 0.5 m and with an antecedent moisture content above 50% would have become unstable under this rainfall (Fig. 9b). According to landslide inventory records (in 't Veld and de Graaf, 1990), Cyclone Bola triggered 547 soil slips along 12 transects within a 3700-ha area. The mean depth of soil slips was 1.1 m and mean slope angle 20–32^0. A 10mm/h-intensity rainfall over 26 hours will cause landslides on slopes over 45^0, with a soil layer-1 0.5.m thick, at 50% antecedent moisture condition (Fig. 9a). This rainfall event is equivalent to a 260 mm total rainfall. If the antecedent moisture level is increased to 80%, the required rainfall duration for instability will be reduced to 10 hours. These estimates are consistent

Table 4 – Worked examples

Example 1 Determine an approximate range of critical rainfall durations for a hillslope in the study area with a slope angle of 30° and a soil layer-1 thickness of 0.5 m at an average rainfall intensity of 8.5 mm/h. The antecedent moisture content is given as 50% saturation.	According to Fig. 7a, for a 35° slope and 0.5-m thickness soil layer-1, the critical shear plane is located in the soil layer-2. Therefore only Fig. 9(a,b) is needed to determine the critical thresholds. The combinations of critical rainfall durations, average uniform rainfall intensity and slope angle for 50% antecedent moisture content in Fig. 9a give an approximate critical rainfall duration of 29 h for 8.5 mm/h average uniform rainfall intensity. This is equivalent to 246 mm total rainfall within 29 h. According to Fig. 9a, hillslopes with soil layer-1 thickness of more than 0.5 m and slope angles steeper than 35° become unstable under these climatic conditions. If the antecedent moisture under the same conditions is increased to 80%, almost all the hillslopes with slope angles of more than 35° and soil layer-1 thickness 0.5 m become unstable within the first 13 hours of the rainstorm.
Example 2 Find the critical slope angle for a hillslope with 0.8m soil layer-1 thickness and 80% antecedent moisture content under a rainfall of 10.5 hours duration at 12mm/h uniform intensity. Then find the approximate range of critical rainfall durations for rainfall intensities from 7 to 14mm/h under the same conditions.	Answer can be obtained by drawing a curve through the intersection point 'c' (x=12mm/h, y=10.5h) on Fig. 9b. This curve is drawn by assuming a linear relationship between the critical rainfall duration and slope angle between 35° and 45°. The approximate critical slope angle for the given set of conditions is 38°. Critical rainfall duration for any rainfall intensity from 7 to 14mm/h can then be found from this drawn curve.

with landslide events recorded in eastern Taranaki hill country where shallow landslides are common during heavy rain (de Rose, 1994). In March 1990, 371 landslides were recorded from a rainfall total of 235mm in 48 hours, and in 1971, 100 landslides were recorded from an event of 227mm in 48 hours. When antecedent moisture conditions were high, such as the period when 85mm of rain over 3 days were followed by an event of 83mm in 48 hours, 91 landslides resulted (de Rose, 1994). These results indicate a reasonable correlation between the model predictions and the observed data.

Conclusion

A simple composite model has been developed to predict the threshold combinations of climatic and topographic (slope angle) variables needed to trigger shallow landslides on tephra-covered hill country in the East Coast region of the North Island. The model parameters can be obtained using relatively quick, simple, inexpensive, but reliable field and laboratory tests. The applicability of the model can be extended to any shallow landslides on infinite hillslopes as long as the Green and Ampt assumptions are valid. The model, coupled with climatic data and other available land resource databases, could provide a suitable basis for determining the long-term risk of catchments or regions to landsliding, and thus provide background information for planning sustainable land use. The approach taken in this paper could be further extended, with integration into a GIS and decision support framework, to assess regional landslide risk.

Acknowledgements

We thank Donna Rowan and Dr Michael Marden for help in the field. Mr John Kirkpatrick is thanked for allowing us to carry out our field experiments on his farm as well as for providing logistical support. We thank Mrs Christine Bezar for editorial assistance. Reviewers of an earlier version of this paper are thanked for their comments. The research on which this paper is based was funded from Foundation for Research Science & Technology Contract C09406.

References

Anderson, M. G.; Howes, S. 1985: Development and application of a combined soil water-slope stability model. *Quaternary Journal of Engineering Geology 18:* 225–236.

Anderson, M. G.; Lloyd, D. M. 1991: Using a combined slope hydrology-stability model to develop cut slope design charts. *Proceedings of Institution of Civil Engineers, 2*: 705–718.

Brakensiek, D. L. 1977: Estimating the effective capillary pressure in the

Green and Ampt infiltration equation. *Water Resources Research, 13(3)*: 680–682.

Bjerrum, L. 1973: Problems of soil mechanics and construction on soft clays and structurally unstable soils (collapsible, expansive and others) in unstable soils. In: *Proceedings of 8th International Conference on Soil Mechanics and Foundation Engineering 3*, 111-159.

Brooks, S.M.; Anderson. M.G. 1995: Determination of suction-controlled slope stability in humid temperature environments. *Geografiska Annaler 77 A(1–2):* 11–22

Brooks, S.M.; Richards, K.S.; Anderson, M.G. 1993: Approaches to the study of hillslope development due to mass movement. *Progress in Physical Geography 17(1)*: 32–49.

Brooks, S.M. Crozier, M.J. Preston, N. 1998. Abstract at 23 European Geophysical Union Meeting , Nice, April 1998. *Annals Geophysicae, Supplement IV*, Vol. 16, Page C1217.

Chandler, R.J. 1988: The *in situ* measurement of the undrained shear strength of clays using the field vane. In Vane shear strength testing, field and laboratory studies. Edited by A. F. Richards. American Society for Testing and Materials, Special Technical Publication 1014: 13–44.

Childs, E. C.; Bybordi, M. 1969: The vertical movement of water in stratified porous material 1. Infiltration. *Water Resources Research 5(2)*: 446–459.

Crozier, M.J. 1969: Earthflow occurrence during high intensity rainfall in Eastern Otago (New Zealand) *Engineering Geology 3:* 325–334.

Crozier, M. J. (Ed.) 1989: *Landslides Causes, Consequences and Environment.* Routledge, New York, 169–192.

de Rose, R., 1994: Effect of rainfall intensity on the spatial density of shallow landslides in a small watershed, Taranaki, New Zealand. In: *Proceedings of the International Symposium on the Forest Hydrology*, Tokyo, Japan, October 1994, 391–398.

Elrick, D.E.; Reynolds, W.D.; Tan, K.A. 1989: Hydraulic conductivity measurements in the unsaturated zone using improved well analysis. *Groundwater Monitoring Review 9*: 184–194.

Eyles, G.O. 1983. The distribution and severity of present soil erosion in New Zealand. *New Zealand Geographer 39*: 12–28.

Fourie, A.B. 1996: Predicting rainfall-induced slope instability. *Proc. Institution of Civil Engineers. Geotechnique.Engng 119:* 211-218.

Green, W.H.; Ampt, G.A. 1911: Studies on soil physics, The flow of air and water through soils. *Journal of Agricultural Science 4(1)*: 1–24.

Gupta, R.K.; Rudra, R.P.; Patni, N.K.; Wall, G.J. 1993: Comparison of saturated hydraulic conductivity measured by various field methods. *American Society of Agricultural Engineers 36(1)*: 51–55.

Hillel, D. 1977: *Computer simulation of soil water dynamics.* International Development Research Council, Ottawa.

in 't Veld, G. J.; de Graaf,F. 1990: *Erosion damage as a result of Cyclone Bola. An assessment on Arai Matawai and Emerald hills properties East Coast region, North Island.* Unpublished report, Forest Research Institute, Ministry of Forestry, Gisborne, New Zealand.

Kao, C.S.; Hunt, J.R. 1996 Prediction of wetting front movement during one-dimensional infiltration into soils. *Water Resources Research 32(1):* 55–64.

Kelliher, F.M.; Marden,M.; Watson, A.J.; Arulchelvam, I.M. 1995: Estimating the risk of landsliding using historical extreme river flood data. *Journal of Hydrology (New Zealand 33(2):* 123–129.

Lambe, T.W. 1951: *Soil Testing for Engineers.* John Wiley, New York.

Lambe, T.W.; Whitman, R.V. 1979: *Soil Mechanics SI version.* John Wiley, New York.

Mein, R.G.; Larson, C.L. 1973: Modelling infiltration during steady rain. *Water Resources Research 9(2):*, 384–394.

Montgomery, D.R.; Dietrich, W.E. 1994: A physically based model for the topographic control on shallow landsliding. *Water Resources Research 30(4):* 1153–1171.

Moore, P.R.; Mazengarb C. 1992: Geology and landforms of Raukumara Peninsula. In Soons, J.M. and Selby, M.J.(Eds.) *Landforms of New Zealand.* 2nd edition. Longman Paul, 334–343.

Murillo, M.L.; Hunter, G.J. 1996: Modelling slope stability uncertainty: a case study at the H.J. Andrews Long-term Ecological Research Site, Oregon. In *Spatial Accuracy Assessment in Natural Resources and Environmental Sciences.* USDA Forest Service General Technical Report RM-GTR-277, 281–290.

Phillips, C.J.; Marden, M.; Pearce, A.J. 1990: Effectiveness of reforestation in prevention and control of landsliding during large cyclonic storms. In *Proceedings of the International Union of Forest Research Organisations 19th World Congress, 5-11 August 1990, Montreal, Canada,* 340–350.

Pradel, D.; Raad, G. 1993: Effect of permeability on surficial stability of homogenous slopes. *Journal of Geotechnical Engineering, 119(2):* 315–332

Rahardjo, T.T.L.; Chang, M.F.; Fredlund, D.G. 1996: Effect of rainfall on matric suctions in a residual soil slope. *Canadian Geotechnical Journal 33:* 618–628.

Watson, A.J.; Marden, M.; Phillips, C.J. 1998: Root strength, growth and rates of decay: a comparative study of the root reinforcement changes of two species and their contribution to slope stability. In: *The Supporting*

Roots: Structure and Function. Proceedings of International Conference, July 20-24 1998, Bordeaux, France.

Whisler, F.D.; Bouwer, H. 1970: Comparison of methods for calculating vertical drainage and infiltration for soils. *Journal of Hydrology 10:* 1–19.

Wolle, C.M.; Hachich, W. 1981: Rain-induced landslides in southeastern Brazil. *Proceedings of the Tenth Conference on Soil Mechanics and Foundation Engineering 3:*1639–1642.